Structural and electrical properties of composites of polymer-iron carbide nanoparticle embedded in carbon

S. Shekhar * V. Prasad, S. V. Subramanyam

Department of Physics, Indian Institute of Science, Bangalore, 560 012, India.

Abstract

The electrical transport properties of composites of polymer and iron carbide nanoparticle embedded in carbon have been studied from 300K to 1.3K. The composites show percolative type behavior with a low threshold value. The XRD shows amorphous nature of the composite. The temperature dependence of conductivity follows two different Efros-Shklovskii variable range hopping mechanisms ($\sigma = \sigma_0 exp[-(T_{ES}/T)^{1/2}]$) with different pre-exponential factors (ρ_0) and different T_{ES} values in range 300K-6K. Thermogravimetric analysis shows that the thermal stability of composites does not depend on filler content to a large extent.

Key words: Polymer composites; Pyrolysis; Transport properties; Nanostructures; Transmission electron microscopy

1 Introduction

Polymer-composites incorporating metal, semiconductor, carbon black, nanomaterials and magnetic materials have been widely used and studied as multifunctional materials with inherent polymer properties. Composites of polymer and magnetic nanoparticles are the subject of extensive research in view of technological importance which varies from high density data storage, electromagnetic shielding, electronic circuitry, switch, sensor to biomedicine [1–3]. Nanoparticles (magnetic) renewed the interest in polymer composites. The properties of nanoparticles differ from those of the same material in bulk due to quantum size effect. The macroscopic properties of composites exhibit

* Corresponding author. Tel.: +91-80-2293-2313; fax: +91-80-2360-2602
Email address: sshekar@physics.iisc.ernet.in (S. Shekhar).

novel properties due to the combined action of quantum size effects, interface between nanostructures and matrix, matrix properties and morphologies of nanoparticle. Polymer embedded with magnetic nanoparticle behaves like an usual magnet without loosing the inherent polymer characteristics of light weight, flexibility and corrosion resistance. These materials have attracted the attention of physicists due to giant Hall effect and giant magnetoresistance [4].

The conductivity of insulating materials like polymers can be enhanced by several orders of magnitude by incorporating some conducting filler in it. The conducting particles make infinitely connected percolative network after a threshold concentration resulting in an enhancement in conductivity by several order of magnitude (6 to 10 order). Above the threshold value (p_c), the conductivity follows the relation $\sigma = \sigma_0(p - p_c)^t$ [5]. The percolation theory predicts the threshold value (p_c) close to 17% for spherical particle systems. Monte Carlo Simulation in three dimensions shows a universal value for critical exponent t (=2). But both universal and non-universal value of t has been observed experimentally and reported theoretically [7,11,13]. The low percolation threshold can be achieved in the case where the fillers have high aspect ratio such as fibres, nanotubes and flakes. The nanomaterials also help in bringing down the threshold value due to its large surface to volume ratio. The threshold value as low as 1 weight% has been reported [12]. The temperature dependence of conductivity of polymer-conductor composites show wide range of conduction mechanism depending on matrix, filler and interaction between filler and matrix. The most common conduction mechanism observed in polymer-conductor composites is variable range hopping ($\rho = \rho_0 exp[T_0/T]^n$; n<1) [14,15]. If the filler particle is relatively bigger in size thermal fluctuation induced tunneling governs the transport properties ($\rho = \rho_0 exp[T_1/(T_0 + T])$ [16,17].

2 Experimental

The filler material which contains iron carbide nanoparticles embedded in carbon matrix are prepared by pyrolysis of maleic anhydride ($C_4H_2O_3$) and ferrocene [$(C_5H_5)_2Fe$)] in 2:1 molecular weight ratio. The pyrolysis is carried out in double zone furnace at 980^0C for $5\frac{1}{2}$ hours in a quartz tube and the yield after the pyrolysis is fine black color soot which contains iron carbide nanoparticles and graphitized carbon (We designate this powder as filler for all future reference in text) [6]. The thin layers of carbon coating over iron carbide has been observed in TEM micrograph (fig.4). The polymer composites are obtained by mixing the filler in different proportions with poly(vinyl) chloride (PVC). The PVC is first dissolved in tetrahydrofuran (THF) and the appropriate proportion of filler is ultrasonicated in PVC for 2 hours to get

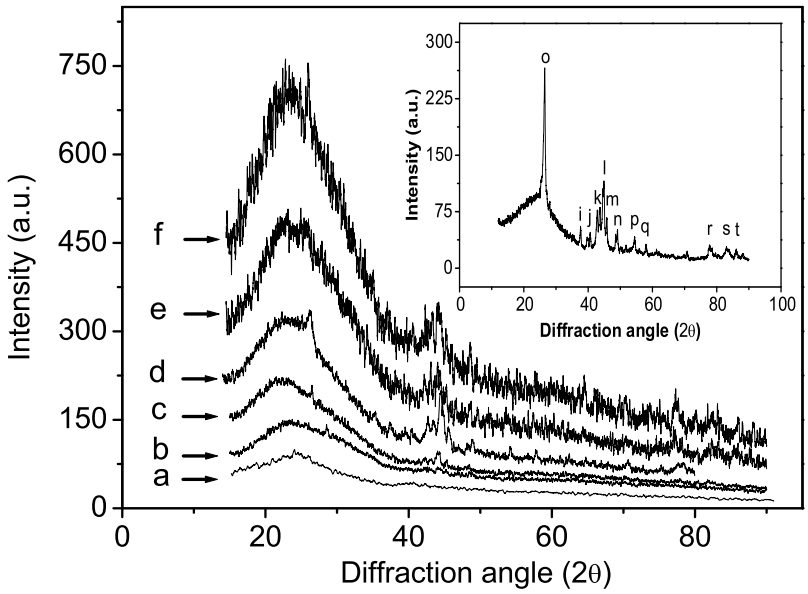

Fig. 1. shows XRD patterns of composites having different proportions of filler. The amount of filler in different composites: (a) has 0 % of filler (pure pvc), (b) 3.2% , (c) 15.5%, (d) 23.1%, (e)25%, (f) 34.8%. Inset shows the XRD patterns of filler (pyrolyzed maleic anhydride and ferrocene at 980^0C). The o peak correspond to graphite 002 plane. The other peaks i (37.76°,112); j (40.99°,120); k (43.91°, 210); l (45.07°, 103); m (46.03°, 211); n (49.2 °, 211); p (54.6°, 004); q (58.06°, 123); r (77.7 °, 401); s (83.1°, 332); t (86.2°, 303); correspond to different planes of iron carbide (Fe_3C). Source JCPDS references.

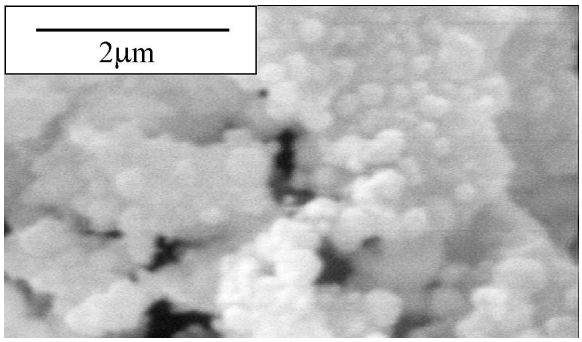

Fig. 2. SEM micrograph of filler. The round shaped particle is carbon coated iron carbide nanoparticle. They are clustered together.

homogeneous dispersion and the solution is allowed to settle in an optically flat beaker [7]. The film thickness is found to be of the order of 100 micrometer. For measurement of resistance four probe method has been used and the contacts have been made by silver paint. Janis liquid Helium cryostat has been used for low temperature transport measurements. Thermal stability of composites are analyzed by PYRIS EXSTAR-6000 thermal analyzer in N_2

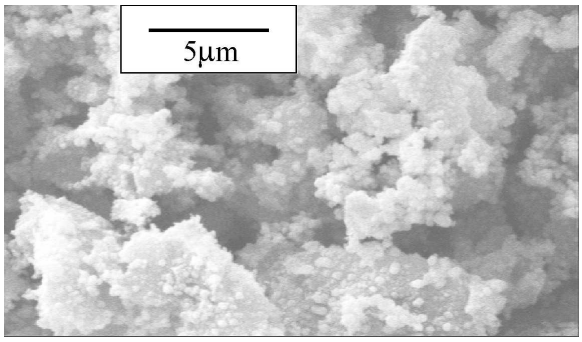

Fig. 3. SEM micrograph of filler at lower magnification. Agglomeration of filler particles are seen.

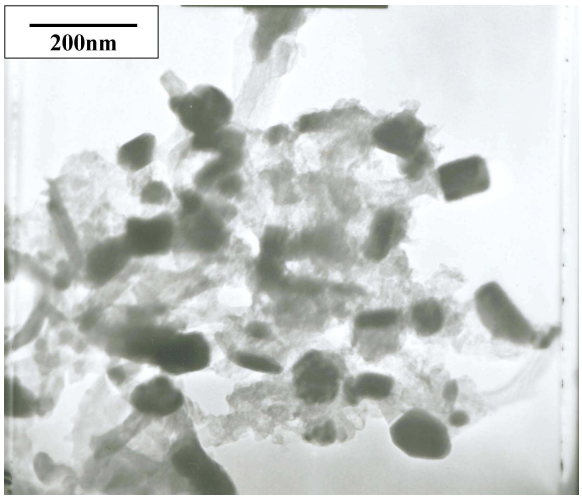

Fig. 4. TEM micrograph of filler material. Most of the iron carbide nanoparticles are approximately 100 nm in size and irregular in shape. Carbon coating over nanoparticle appears light black in color.

environment. The rate of heating has been kept 5°/minute with nitrogen flow rate of 150ml/minute.

The structure and different phases of C:Fe in filler as well as in composite are identified by X-ray diffraction of wavelength 1.5406 $\mathring{A}$. The XRD pattern shows (see fig. 1) graphitized carbon and Fe_3C phases present in the filler. Using Scherer formula, crystallized size of graphitized carbon from XRD pattern (fig.1) is calculated to be 14.34 nm.

SEM is done on the samples to get the distribution of filler inside the composite and its surface morphology. The shape and size of the particles are determined by transmission electron microscopy (TEM). The SEM graphs (fig.2 and 3) show the agglomeration of particles (filler). There are grains of nearly (less than) 100 nm size of iron carbide coated by graphitized carbon as seen in TEM micrograph (fig. 4).

3 Rsesult and discussion

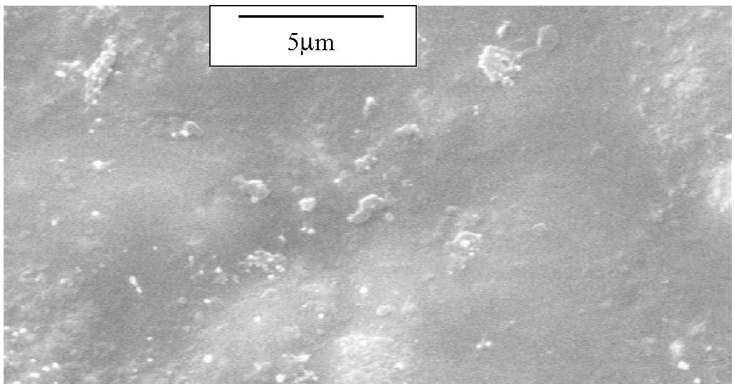

Fig. 5. SEM figure of composite, filler content 15.4%. The tiny shining spots are filler particles.

3.1 Structural properties

The broad peak in XRD pattern of composites (fig.1) reveal amorphous nature. Also few crystalline peaks appeared in heavily filled composites. The peak nearly at 26^0 is of graphitized carbon present in filler material whereas peak at 45^0 is due to presence of iron carbide in it. For heavily filled composites peak position at 45^0 is more pronounced. SEM (fig.5) of composite shows a homogeneous dispersion of filler particles in polymer matrix at micrometer scale. The bright dots seen in the SEM (fig.5) micrograph are filler particles.

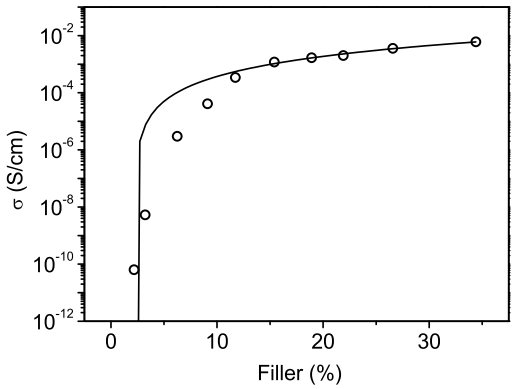

Fig. 6. shows variation of conductivity of composite as a function of filler concentration by weight. There is a sudden rise in conductivity at 2.2 weight % of filler concentration.

3.2 DC conductivity

Fig. 6 shows the plot of conductivity of composites at different concentration of filler. The insulator-conductor composites form a percolative path for conduction and conductivity follows the equation

$$\sigma = \sigma_0(p - p_c)^t \tag{1}$$

There is a steep rise in conductivity as the concentration crosses p_c (percolation threshold). Fig. 6 shows the enhancement in conductivity above particular value of filler concentration. By fitting equation 1 in the experimental data the value of percolation threshold (p_c) and critical exponent (t) have been obtained as 2.2% (by weight) and 1.96 respectively. The threshold value is low whereas the critical exponent matches with the theoretically predicted value of t=2 in three dimensions. In our previous report on polymer amorphous carbon composites [7] the critical exponent value was found to be 3.1. In that case the host matrix (polymer) was same but conducting particle size was much larger (micrometer and irregular in shape). In fact t depends on the filler particles shape and size [10] and a systematic study has to be done in this direction. The non universal value of t and low threshold have been observed earlier also [11]. The non universal value is also theoretically predicted by Balberg for a non touching percolative network [13].

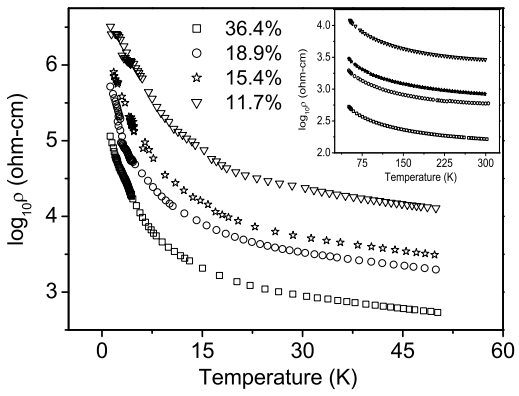

Fig. 7. The Fig. shows the temperature dependence of resistivity of nanoparticle composites from 1.2K-50K. Inset Fig. shows the temperature dependence from 50K-300K.

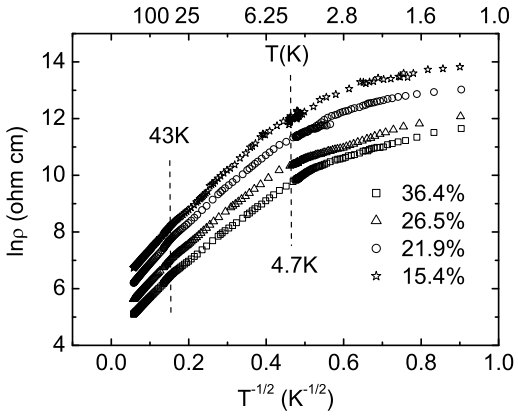

Fig. 8. The Fig. shows the plot of lnρ vs. $T^{-1/2}$.Two crossovers have been estimated at 43K and 4.7K. With more careful analysis crossovers are found at 55K and 4.7K.

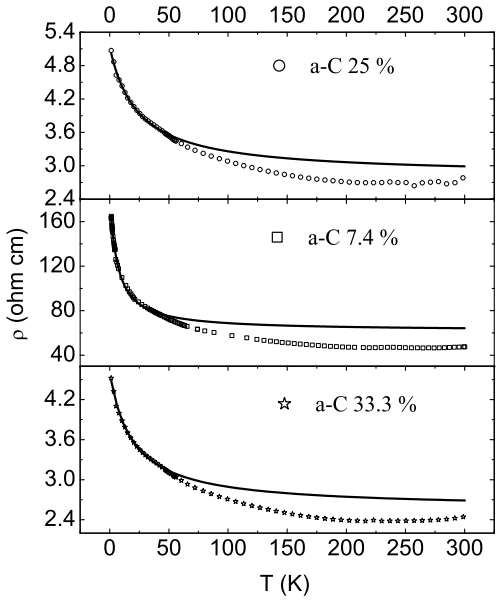

Fig. 9. The Fig. shows the temperature dependence of polymer-carbon (amorphous) composites. Symbols are the experimental data points and corresponding solid line is the fit of equation 2. This Fig. is adapted from reference[7], curtsey Elsevier Science.

3.3 Temperature dependence of resistivity

Fig. 7 shows temperature dependence of resistivity of nanoparticle composites. The change in resistance is nearly four orders of magnitude as temperature dips from room temperature to 1.3K. The conductivity of polymer-conductor

composites usually follow the three type of conduction mechanisms namely thermal fluctuation induced tunneling, granular metal conduction and variable range hopping conduction.

Thermal fluctuation induced tunneling conduction is due to Sheng [16,17] and the conductivity follows the equation

$$\sigma = \sigma_t exp[-T_1/(T + T_0)] \tag{2}$$

where σ_t, T_0 and T_1 are constants which depends on the junction formation, filler shape and size and matrix used. In this model conducting islands are separated by insulating material, form junction. The charge carriers tunnel through this junction by a potential difference which is produced due to local thermal fluctuation [16]. This mechanism is followed by the composites which is usually filled with micrometer size of particles [18]. In this case formation of real junction is possible.

Many of the cases of polymer-conductor composites obey the conduction mechanism for granular metal and follow the equation [19]

$$\sigma = \sigma_g exp(-b/T^{1/2}) \tag{3}$$

The granular metal is a dispersion of fine metallic particle in dielectric matrix. Electrical conduction in granular metals is due to transfer of charge carriers from charged grains to neutral grains separated by dielectric material. Generation of charge carriers (electron or holes) require a minimum amount of energy E_c=(e^2/d)F(s/d) which depends on grain size (d), separation between grains (s) and the function F depends on shape and distribution of grains [19].

The most common conduction mechanism followed by polymer composites and other disordered semiconductor is variable range hopping (VRH) conduction given by equation

$$\sigma = \sigma_v exp[-(T_v/T)^n] \tag{4}$$

where σ_v has weak temperature dependence (σ_v=BT^{-m}) and may be regarded as constant. The values of n varies between 1/4 and 1. The value of n depends on the behavior of density of states near the Fermi energy. If density of states (DOS) g(E) varies as $g_0 \mid E - E_F \mid^m$ near to Fermi level then n can take the value (m+1)/(m+4) [20]. When DOS is constant equation 4 takes the form of Mott's VRH with exponent (n) equaling 1/4. In case of quadratic dependence of DOS, equation 4 represents Efros-Shklovskii VRH with exponent 1/2. VRH kind of conduction mechanism has been observed in polymer-conductor composite systems [15]. The vanishing DOS (quadratic dependence; m=2) near

to Fermi level is produced due to coulomb interaction between the hopped electron and hole created at hopped site. This gives rise to a coulomb gap near to Fermi level and the systems obey ES-VRH [14].

The disordered metallic behavior have been also observed in few of the highly conducting composites having large fraction of filler material [21]. In the carbon black-polymer composite studied by Dawson et. al.[21] the conductivity shows the characteristic of two dimensional disordered metal and at low temperatures it follows the relation $\sigma\alpha$ lnT.

The temperature dependence of resistivity of the composites follows Efros-Shklovskii variable range hopping (ES-VRH) from 300K-55K and 34K-6K with different coulomb gaps (see fig. 8) (The fig. shows transition at 43K and 4.7K but with more careful analysis the range was found to be 300K-55K and 34K-6K) [8]. Below this temperature another crossover occurs and resistivity shows linear dependence on temperature [8]. The conductivity of composites differ from the filler even at 36.4% of filler concentration. The filler here shows semiconducting behavior and resistance depends linearly on logarithmic (natural) of temperature [9]. Previously we have reported the transport properties of polymer-carbon (amorphous) composites [7] and found that thermal fluctuation induced tunneling (eq.2) governs the conduction mechanism at low temperatures. In that case the filler (carbon particles) of micrometer size ($\sim 40\mu$) were dispersed in PVC. The conduction mechanism in amorphous carbon composites and nanoparticle composites differ completely. In amorphous carbon polymer composites thermal fluctuation induced tunneling (eq.2) is followed from 1.3K to 50K-60K. Due to different thermal expansion coefficient between carbon and polymer, the gap between conducting carbon increases that suppresses tunneling conduction. At higher temperature two effects act simultaneously; the differential thermal expansion between carbon and polymer which reduces the tunneling conduction and higher thermal energy which provides more tunneling current. Due to these combined effects in large temperature range (150K-250K) not much change in resistance has been observed (see fig. 9) [7]. Finally near to room temperature resistance started increasing because differential thermal expansion overcomes tunneling conduction (positive temperature coefficient of resistivity). This behavior is absent in nanoparticle composites. There is no such effect of positive temperature coefficient at room temperature is observed. In nanoparticle-polymer composites filler is very fine (soot) and so they are very large in number. The separation between particles are very less. So the effect of differential thermal expansion is minimal and conduction mechanism is solely variable range hopping. The change in resistance ($\rho(1.3K)/\rho(300K)$) for nanoparticle composites is found to be few orders of magnitude whereas in amorphous carbon composites the change observed is nearly an order and less. Quantitatively the nanoparticle composites are more disordered.

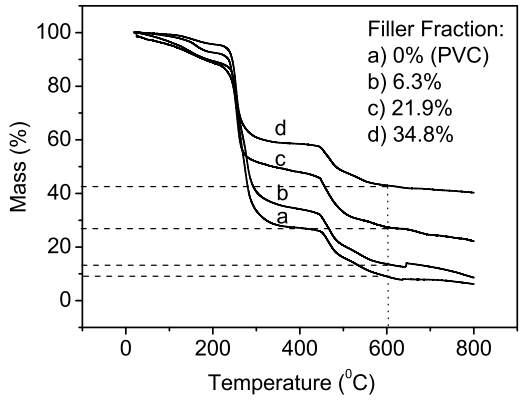

Fig. 10. TG curves of polymer-composites. Degradation of composites starts at 250°C.

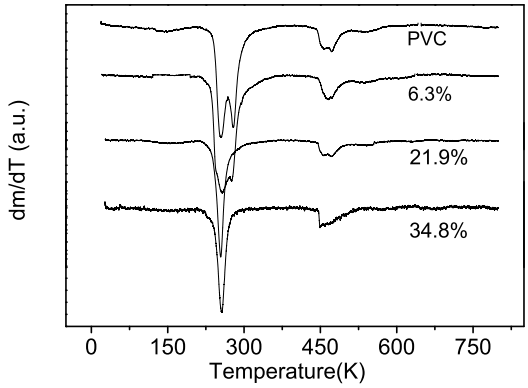

Fig. 11. DTA curves of polymer-composites. Rate of massloss is high at nearly 250° and 450°C.

3.4 Thermal analysis

Thermogravimetric analysis (TGA) is one of the powerful tools to determine the stability of polymer-composites. In some cases, by the method of TGA one can estimate the filler fraction in host material. The TGA and Differential thermal analysis (DTA) of three of the samples and pure PVC are shown respectively in fig. 10 and 11. The degradation of composites starts at 250°C and there is again a rapid change in mass occurs nearly at 450°C. The TGA and DTA behaviors of composites are very similar to host material (PVC) [22]. Pure PVC decomposes completely at 550°C and residue remains as carbon. At 600°C the remain of the composite is higher than the filler percentage. This is due to the fact that the filler as well as residue of the PVC remain there. The dm/dT becomes very sharp near to 250° as the concentration of filler is increased. The presence of filler particles narrow the degradation range near

to 250°C.

4 Summary and Conclusions

The low temperature (300K-1.3K) transport properties of composites of polymer-iron carbide nanoparticle embedded in carbon have been studied. The composite establishes a percolative path when filler concentration crosses 2.2% by weight and dc conductivity follows the scaling law $\sigma=\sigma_0(\text{p-p}_c)^t$. The XRD pattern shows disordered nature of the materials. ES-VRH mechanism of conduction is followed in two different temperature segments (300K-55K and 34K-6K). It has been found that low temperature electrical transport depends on particle size. If particle size is large (micrometer) thermal fluctuation induced tunneling is the conduction mechanism whereas in nanoparticle composites VRH mechanism is followed. The thermogravimetric analysis shows that there is not much effect on the stability of the host by the inclusion of filler.

Acknowledgements: We wish to acknowledge the Sophisticated Analytical Instrument Facility (SAIF) and Ms. Bharati, I.I.T. Bombay for doing TEM. Department of Science of Technology, New Delhi is acknowledged for providing the National Low Temperature and High Magnetic Facility at I.I.Sc. Bangalore where this work has been performed. Authors would like to acknowledge all the lab-mates for their constant support. We are thankful to Ms.E.P.Sajitha for some fruitful discussions. One of us (S.S.) is grateful to CSIR, New Delhi for granting the scholarship.

References

[1] J. L. Wilson, P. Poddar, N. A. Frey, H. Srikanth, K. Mohomed, J. P. Harmon, S. Kotha,J. Wachsmuth, J Appl. Phys. 95 (2004) 1439.

[2] Q. A. Pankhurst, J. Connoly, S. K. Jones, J. Dobson, J. Phys. D 36 (2003) R167.

[3] N. Guskos, E. A. Anagnostakis, V. Likodimos, T. Bodziony, J. Typek, M. Marynaik, U. Narkiewicz, Kucharewicz, J. Appl. Phys. 97 (2005) 0243041.

[4] A. E. Varfolomeev, D. Y. Godovskii, G. A. Kapustin, A. V. Volkov, M. A. Moskvina, JETP Lett. 67 (1998) 39.

[5] S. Kirkpatrick, Rev. Mod. Phys. 45 (1973) 574.

[6] E. P. Sajitha, V. Prasad, S. V. Subramanyam, S. Eto, K. Takai, T. Enoki, Carbon 42 (2004) 2815.

[7] S. Shekhar, V. Prasad, S. V. Subramanyam, Carbon 44 (2006) 334.

[8] S. Shekhar, V. Prasad, S. V. Subramanyam, (submitted).

[9] E. P. Sajitha, V. Prasad, S. V. Subramanyam, (submitted).

[10] F. Carmona, P. Prudhon, F. Barreau, Solid State Comm. 51 (1984) 255.

[11] S. I. Lee, Y. Song, T. W. Noh, X. Chen, G. R. Gaines, Phys. Rev. B 34 (1986) 6719.

[12] P. Mandal, A. Neumann, A. G. M. Jansen, P. Wyder, R. Deltour, Phys. Rev. B 55 (1997) 452.

[13] I. Balberg, Phys. Rev. Lett. 59 (1987) 1305.

[14] B. I. Shklovskii, A. L. Efros, Electronic Properties of Doped Semiconductors, Springer-Verlag, Berlin, 1984.

[15] D. vanderPutten, J. T. Moonen, H. B. Brom, J. C. M. Brokken-Zijp, M. A. J. Michels, Phys. Rev. Lett. 69 (1992) 494.

[16] P. Sheng, E. K. Sichel, J. I. Gittleman, Phys. Rev. Lett. 40 (1978) 1197.

[17] P. Sheng, Phys. Rev. B 21 (1980) 2180.

[18] F. Carmona, Physica A 157 (1989) 461.

[19] P. Sheng, B. Abeles, Y. Arie, Phys. Rev. Lett. 31 (1973) 44.

[20] E. M. Hamilton, Philos. Mag. 26 (1972) 1043.

[21] J. C. Dawson, C. J. Adkins, J. Phys.: Condens. Matter 8 (1996) 8321.

[22] D. A. Skoog, F. J. Holler, T. A. Nieman, Principle of Instrumental Analysis, 5th Ed., Harcourt Asia Pte Ltd., Singapore, 1998.